# Application of green-synthesized carbon dots for imaging of cancerous cell lines and detection of anthraquinone drugs using silica-coated CdTe quantum dots-based ratiometric fluorescence sensor

**Arash Mohammadinejad**
Mashhad University of Medical Sciences
**Khalil Abnous**
Mashhad University of Medical Sciences
**Morteza Alinezhad Nameghi**
Mashhad University of Medical Sciences
**Roghayeh Yahyazadeh**
Mashhad University of Medical Sciences
**sara hamrah**
Mashhad University of Medical Sciences
**Fereshteh Senobari**
Mashhad University of Medical Sciences
**Seyed Ahmad Mohajeri** ( mohajeria@mums.ac.ir )
Mashhad University of Medical Sciences

**Method Article**

**Keywords:** Carbon dots, CdTe quantum dots, Daunorubicin, Doxorubicin, Ratiometric method, Imaging

**Posted Date:** May 27th, 2022

**DOI:** https://doi.org/10.21203/rs.3.rs-1668426/v1

# Abstract

**Background:** Daunorubicin and doxorubicin, as chemotherapy drugs, treat cancer with many side effects. Therefore, detection of them in the biological system for regulation and controlling of usage is essential.

**Results:** In this way, a ratiometric fluorescent method was designed for quantification of daunorubicin and doxorubicin using bell pepper-based carbon dots, as variable signal, and silica-coated CdTe quantum dots, as an internal reference. The detection was performed based on variations of carbon dots intensity in the presence of daunorubicin and doxorubicin concentrations in comparison with the constant intensity of silica-coated CdTe quantum dots. The proposed ratiometric fluorescent method was successfully used for detection of daunorubicin and doxorubicin range of 54.37-8156.6 nM and 86.2-17242 nM, with a detection limit of 18.53 and 29 nM, respectively. In addition, this method was used for detection of drugs in serum samples with recovery ranges of 86.14-99.62 (RSD 3-1.47%) and 86.32-97.53 (3.38-1.48%), respectively. Finally, after evaluation of carbon dots by MTT test, applicability of carbon dots was checked to image prostate cancer cell lines (PC-3) and breast cancer cell lines (MCF7).

**Conclusions:** The results demonstrated that despite improvement of the repeatability and interferences reduction by ratiometric method, also carbon dots successfully used for imaging of cell lines.


# 1. Introduction

Carbon quantum dots (CDs), as a new and fascinating class of fluorescent nanomaterial with a size below 10 nm, have recently gained considerable attention of scientists due to their unique properties in comparison with other traditional quantum dots. Several properties for these nanoparticles can be mentioned such as biocompatibility, photostability, low toxicity, eco-friendly, water solubility and strong fluorescence[1, 2]. Heretofore, a wide range of methods including plasma[3], laser ablation[4], arc discharge[5], electrochemical[6], hydrothermal[7], acidic oxidation[8], ultrasonic[9] and microwave treatment[10] have been reported for synthesis of CDs. Recently, hydrothermal method using natural resource materials as precursors has been developed for preparation of CDs. In this context, several natural resources such as oranges[11], potatoes[12], hair[13], watermelon peels[14], bananas[15], milk [16], coffee [17], honey[18], ginger juice[19], orange waste peels[20], and pomegranate fruit[21] have been employed for development of a simple, low cost, and green synthesis method.

Anthracycline anticancer antibiotics, such as doxorubicin (DOX) and daunorubicin (DAN), are widely applied to treat cancers such as breast, lungs, ovarian, bladder, acute lymphocytic leukemia, prostate, and neoplastic disease [22–24]. Nonetheless, utilizing these drugs at the concentrations above-allowed level in blood may lead to tissue necrosis, marrow suppression, cardiac toxicity, and oral ulcers [23, 25]. So, due to the toxicity effects of these drugs, the development of sensitive and simple analytical techniques is of great importance to clinical research. In recent years, several methods such as liquid chromatography [26], electrochemistry [27], spectrophotometry [28], fluorescence [24], Raman scattering

[29], and resonance rayleigh scattering [30] have been employed for quantification of anthracycline antibiotics.

Among the aforementioned methods, single wavelength fluorescence sensors, as the subset of the fluorescence method, have been of great interest in analytical methods for anthracycline drugs [24, 25, 31] due to their advantages, such as simplicity and sensitivity. Unfortunately, some analytical errors arising from inconstancy in concentration, environment, and excitation source have limited their usage [32, 33]. Ratiometric fluorescent (RF) sensors with a built-in correction factor can effectively remove these problems. So, RF sensors, in which emission ratios do determinations at two different wavelengths, enhance precision, accuracy, and sensitivity [34].

This research reported quantification of DOX and DAN using RF sensors designed by green synthesized CDs and silica-coated CdTe quantum dots (Si@CdTe QDs) in serum samples. The quantification was done based on variations of fluorescence intensity (FI) of CDs compared to constant FI of Si@CdTe QDs. Moreover, CDs were employed to imaging breast cancer (MCF7) and prostate cancer cell line (PC3). CDs were synthesized by hydrothermal method from green bell pepper. Based on our knowledge, the application of green synthesized CDs, from green bell pepper, in imaging of aforementioned cell lines and RF sensor for determination of DOX and DAN has not been reported.

# 2. Experimental

# 2.1 Materials

All experimental reagents were of analytical grade. Calcium chloride hexahydrate ($CaCl_2.2.5H_2O$), 3-Aminopropyl triethoxysilane (APTES), tetraethyl orthosilicate (TEOS), mercaptosuccinic acid (MSA), Sodium tellurite ($Na_2TeO_3$), sodium borohydride ($NaBH_4$), ethanol absolute, dimethyl sulfoxide (DMSO), ammonium hydroxide ($NH_4OH$), acetonitrile ($C_2H_3N$), sodium chloride (NaCl), potassium chloride (KCl), sodium hydrogen phosphate ($Na_2HPO_4$), monopotassium phosphate ($KH_2PO_4$), Copper(II) sulfate ($CuSO_4$), magnesium chloride hexahydrate ($MgCl_2.6H_2O$), Potassium nitrate ($KNO_3$), L-Glutamine, Potassium carbonate ($K_2CO_3$) was purchased from Merck. Doxorubicin (DOXO-cell) and Daunorubicin (Injection 20mg) were purchased from Pfizer. Bell pepper was purchased from a local vegetable market in Mashhad. Phosphate Buffered Saline (PBS) containing $Na_2HPO_4$ (14.4 g), KCl (2g) NaCl (80g), KH2PO4 (2.4g) was prepared in deionized water (1 L). Then PH was adjusted at 7.4 with HCl and NaOH solution. Afterward, PBS buffer was sterilized by autoclave.

# 2.2 Instrument

BioTek Microplate Reader (Synergy™ H4 Hybrid Reader, USA) was used for recording UV–Vis absorption and fluorescence spectra. The appearance and size of CDs were measured by transmission electron microscopy (TEM) (LEO 912AB, 120kv, Germany). The crystalline phases of C-dots was performed by a GNR (Italy) X-ray diffractometer (XRD). LEO VP 1450 (Germany) Field Emission Scanning Electron

Microscopy (FE-SEM) was applied to obtain energy-dispersive X-ray (EDX) spectrum of nanoparticles. PerkinElmer spectrophotometer (Version 10.4.4, USA) was used to record fourier transform infrared (FT-IR) spectra in the region. The zeta potential of samples was calculated by Malvern Panalytical dynamic light scattering (DLS) apparatus (UK). The imaging of cell lines was performed by JuLI™ fluorescence microscopy (from NanoEnTek Company).

## 2.3 Synthesis of CDs

A different source of protein [35], ascorbic acid or carbohydrate [36] has been used to synthesize the CDs via various methods. In this study, a green bell was selected to synthesize CDs duo to high-quality contents such as carotenoids, ascorbic acid, carbohydrate, and other carbonaceous organic materials, according to a typical, simple, and one-pot green synthesis method. Firstly, a few bell peppers were sliced, and after separation of seeds, fragmented to several small spices and ground by a juicer. Then obtained paste was added to 100 ml of double distilled water, and the mixture was transferred into an stain steel less autoclave reactor, tightly closed, and heated at 200℃ for 6 h. Afterward, the autoclave cooled down to room temperature, and the dark solution was centrifuged at 4000 rpm for 10 min to eliminate large particles. Finally, the resultant was filtered by 0.45 μm and 0.22 μm syringe filter, freeze-dried, and the resulted powder, which was highly soluble in water, kept at -20℃ in the dark for later use. A proper amount of obtained powder was dissolved in 10 ml of deionized water for the daily administration of was kept at 4 ℃.

## 2.4 Synthesis of MSA-CdTe QDs

The synthesis of MSA-capped CdTe QDs (MSA-CdTe QDs) was done according to our previous studies using a simple and one-pot method without preparation and inner pressure adjustment [37, 38]. To obtain MSA-CdTe QDs, $CdCl_2$ (20 mg,), MSA (45 mg) and $Na_2TeO_3$ (4.4 mg) was mixed with 100 ml borate–acetic acid buffer solution (PH = 7). It was performed in a one-neck flask and vigorously stirring for 10 min. Then $NaBH_4$ (45 mg) was added rapidly and vigorously stirred for another 10 min. The reaction solution was refluxed at 100℃ for 24 hours under outdoor conditions. After slowly cooling and ethanol adding, MSA-CdTe QDs were sedimented by centrifugation at 8500 rpm. Finally, resultant nanoparticles were dissolved in double-distilled water (20 mL) and were kept at 4℃ under dark-condition.

## 2.5 Synthesis of silicate coating on MSA-CdTe QDs

To create Si@CdTe QDs, MSA-CdTe QDs (2 ml) and APTES (60 ml) were added to ethanol (3 ml) in a falcon. After stirring for 30 min, TEOS (270ml) and ammonium hydroxide ($NH_4OH$) (300 ml) were added to this solution and were stirred for 24 hours. The final solution was washed with methanol, and dried powder was kept under dark-condition.

## 2.6 Analytical protocol

In this study, the experimental process was based on emission fluctuation of CDs (in the presence of DOX and DAN) at 450 nm compared to constant emission of MSA-CdTe QDs at 550 nm, which was proportional to the concentration of the anticancer drug. The measurement was done by incubation of

several concentrations of DOX and DAN, CDs (30 ppm), Si@CdTe QDs (12500 ppm) in the 200 µl aqueous medium after 40 minutes. Then emission wavelength was read by Synergy™ H4 Hybrid reader in 400–700 nm. The calibration curve was plotted according to the signal changes of (F0-F)/F0. F0 and F are fluorescence intensity at 450 nm in the absence and presence of the drug, respectively, which is divided on fluorescence intensity at 550 nm. The data were reported as means ± SD. Relative standard deviation (RSD %) was used as a repeatability factor for four repetitions.

# 2.7 Preparation of human serum samples

Blood samples of healthy volunteers were collected from the clinical laboratory in Mashhad. Then the serum sample was obtained by centrifuge at 10000 rpm for 10 min. Due to the high protein of serum, it was deproteinized by acetonitrile (ACN: serum 1:1) according to reference [39, 40]. After 5 min shaking, it was centrifuged at 10,000 rpm at 4 ℃ for 10 min. The resultant was filtered two times. The solution was heated at 60 ℃ to acetonitrile removal, and the pellet was diluted 25 times with PBS. Different concentrations of drugs (DAN and DOX), CDs (30 ppm) and Si@CdTe QDs (12500 ppm) were incubated with blood serum (200 mL) for 40 min.

# 2.8 Cell culture

PC-3 cells (human prostate cancer cell line) and MCF-7 (human breast cancer cell line) were provided from the Pasteur Institute of Iran. Cells were cultured after washing with PBS (×1) and trypsinization for each passage with RPMI 1640 containing 100 units/mL penicillin-streptomycin and 10% heat-inactivated FBS. The culture flasks were kept in a humid atmosphere at 37°C and 5% $CO_2$.

# 2.9 MTT assay

Cytotoxicity of CDs was evaluated by the MTT assay, which is based on the ability of live cells to convert tetrazolium salt MTT to formazan crystals by mitochondrial enzymes [41]. Cytotoxicity of CDs was evaluated by the MTT assay based on the ability of live cells to convert tetrazolium salt MTT to formazan crystals by mitochondrial enzymes. Briefly, cells ($1 \times 10^4$) were seeded in 96-well plates; consequently, the cells were treated with different concentrations (5, 10, 50, 100, 500, 1000, 1500 ppm) of the CDs and incubated at 37℃ and 5% $CO_2$ flow for 24 h. The untreated cell was proposed as a control group. After replacing the new medium in the wells, MTT (10 µL of 5 mg/mL) was added to the wells and incubated at 37℃ in dark conditions for 4 h. Thereafter, the medium was thrown away and replaced with DMSO (100 $\mu$L). The viability of cells was checked by determining the absorption difference in each well at 570 and 630 nm.

# 2.10 Fluorescence imaging

PC-3 and MCF7 cells ($5\times10^4$) were placed in 24-well. After 24 h incubation at 37°C, the culture wells medium was replaced by an RPMI1640 without FBS (500 $\mu$L) containing different concentrations of CDs. Then cells were incubated at 37°C and dark condition for three h. Finally, after deeply wells washing with PBS, the result was analyzed by fluorescence microscopy [42].

# 3. Result And Discussion

# 3.1 Mechanism of synthesis

It is suggested that the probable mechanism of fluorescent CDs production is associated with the carbonaceous natural organic contents in bell pepper. Although the mechanism of CDs formation is still vague but the possible mechanism can be related to the sequential events of dehydration, fragmentation and condensation of carbonaceous contents which may be followed by aromatization and carbonization (**Schematic 1**) [43]. The sugar content is an important factor for formation of CDs. The hydrothermal condition leads to hydrolysation of sucrose to glucose and fructose. Moreover, glucose can be isomerised to fructose. Afterwards, the dehydration and decomposition processes of fructose and glucose take place to form furfural compounds and some organic acids such as citric acid and ascorbic acid, which are able to control dehydration and decomposition processes. In the following, resulted products polymerized and condensed to form soluble polymers, which aromatized to clusters during aldol condensation, cycloaddition and hydroxymethylation of furan compounds. Finally the resulted aromatic clusters saturated leading to nucleation of CDs [11].

# 3.2 Characterization of CDs

According to the UV-Vis absorption spectrum (Fig. 1A), the excitonic absorption peak of CDs was appeared at 300–700 nm wavelengths. Moreover, using the fluorimetry technique, the maximum emission intensity of CDs was recorded at 450 nm wavelength (Fig. 1A). It is necessary to mention, as it is obviously shown under room light, the CDs solution was appeared light yellow, but under UV light, it was seen blue color (**inset**). Characterization and size distribution of CDs with red emission was obtained via TEM. As shown in Fig. 1B, the size of synthesized CDs was estimated smaller than five nm. In addition, in this study, EDX was used to verification of CDs ingredients. According to the pattern (Fig. 1C), composition mainly contained carbon, oxygen and nitrogen. The functionality of the CDs surface was analyzed by FT-IR spectroscopy. According to Fig. 1D, the absorption bands of the functionalization group of hydroxyl viewed at 3381.3 $cm^{-1}$ (υ OH) and 1073.6 $cm^{-1}$ (δ OH). Also, carboxylate (υ $COO^{-}$) presented absorption bands at 1603.9 $cm^{-1}$ and 1407.5 cm-1 related to asymmetric and symmetric vibrations. Also, the absorption band at 2929.6 $cm^{-1}$ is related to C-H [44]. In addition, the zeta potential of the synthesized CDs was obtained − 17.6 mv (Fig. 1E) by DLS, which proved that CDs have carbocyclic acid groups on their surface.

The CDs crystal structure and purity of it was studied by XRD analysis. As it is shown in Fig. 1F, the prominent diffraction peaks were located at 2$\theta$ values of 19.72° (200), 21.90°(001), 44.49° (002), 76.39° (512) matching to the crystal plane of carbon with Entry number 01-080-5332

# 3.3 Si@CdTe QD characterization

The characterization of red emission MSA-capped CdTe QDs was done in our previous study [38]. The fluorescence spectra of MSA-capped CdTe QDs and Si@CdTe QDs are shown in Fig. 2**(A)**. The difference between emission peak position before (600 nm) and after (540 nm) silanization is due to elimination of shallow trap defects and reduction of passivation on QDs surface leading to blue shift [45]. Elemental analysis of Si@CdTe QDs by EDX (Fig. 2C) showed that the main element was Si demonstrating successful coating of the silicate polymer around the CdTe QDs. The evolution of the functional groups of Si@CdTe QDs by FT-IR spectroscopy (Fig. 2D) revealed that the stretching vibration peak at 1058.7 $cm^{-1}$ is attributed to asymmetric vibrations of (O-Si-O) and the stretching peak at 786 $cm^{-1}$ are attributed to symmetric vibrations of (O-Si-O). It is necessary to mention that the bending vibration peak of N-H amide was 1560.3 $cm^{-1}$ and the stretching vibration peak of (C = O) and (O-H) were 1638.2 cm-1 and 3167.3 $cm^{-1}$.

# 3.4 Optimization

In order to optimization of ratiometric detection of DOX and DAN, different conditions such as concentrations of CDs, incubation time and PH of reaction were optimized. For this reason, the intensity changes of different concentrations of CDs (7, 15, 30, and 60 mg/L) were studied in the presence of (2718.8 nM and 5172 nM) DAN and DOX. It is necessary to mention that $F_0$ = (450/550) and F = (450/550) ratio belonged to the fluorescence intensity of the CDs (450 nm) and Si@CdTe QDs (550 nm) nanohybrid system, which adjusted in the absence and presence of drugs, respectively. As shown in Fig. 3**(A)** variations of $(F_0\text{-}F)/F_0$ reached a plateau in 30 mg/L of CDs under condition of PH 7 and 30 min incubation time. So due to the best sensitivity at 30 ppm, this concentration was considered as an optimized concentration for further tests.

The optimization of PH was done by evaluation of RF sensor operation in PBS (0.01 mM) as reaction media. Variations of fluorescence intensity for the RF sensor was probed over the pH range of 6.5- 8 under condition of 30 mg/L CDs, and 30 min incubation time. As shown in Fig. 3**(B)** variations reached to maximum at PH 7 demonstrating the reaction between drugs and CDs completed. As a result, PH 7 chosen as the optimal pH for the detection of DOX and DAN.

Reaction time as a main effective on the fluorescence intensity were surveyed. The effect of incubation time was examined at 5 min intervals during one hour under condition of 30 mg/L CDs, and PH 7. The results revealed (Fig. 3C) that the maximum reduction of emission intensity of CDs was obtained during 40 min demonstrating reaction was completed at 40 min. So 40 min was considered as the best optimization time for incubation.

# 3.5 Detection of DOX and DAN

The response of the introduced ratiometric sensor to increasing the concentration of DOX and DAN was investigated under the beforementioned optimal condition. According to Fig. 3 **(D and F)**, the addition of various concentrations of drugs led to a decrease of fluorescence intensity of CDs while fluorescence intensity of Si@CdTe QDs was constant. As shown in Fig. 3 **(E and G)**, the calibration curves based on

variations of $(F_0\text{-}F)/F_0$ versus logarithmic concentration of drugs were linear in the range of 54.37-8156.6 nM for DAN with LOD of 18.53 nM and 86.2-17242 nM for DOX with LOD of 29 nM. Based on summarized data mentioned in Table 1, it was obviously demonstrated that the sensitivity of the introduced ratiometric sensor is acceptable in comparison with other studies. It should be noted that the intra-day and inter-day (RSD%, n = 3) repeatability values for detection of 862 nM of DOX were 2.31% and 3.96%, respectively. Moreover, these values for detection of DAN were 2.08% and 4.7%, respectively.

Table 1
Comparison of introduced RF sensor in this study with other sensors

| Drug | Linear range | Limit of detection | Analysis method | Ref. |
|---|---|---|---|---|
| DOX | 0.05–4.0 µg/mL (91–735 nM) | 0.002 µg/mL (3.67nM) | multi-walled carbon nanotubes modified platinum electrode (Pt/MWCNTs) | [46] |
| DOX | 70–$5\times10^5$ nM | 9.0 nM | ZnO nanoparticle/1-butyl-3-methylimidazolium tetrafluoroborate modified carbon paste electrode (ZnO-NPs/BMTFB/CPE) | [47] |
| DOX | 0.010–15 µM | 10 nM | nitrogen-doped reduced graphene oxide (N-rGO) suspended in chitosan-modified gold electrode | [48] |
| DOX | 50– 400 nM | 13.8 nM | molecularly imprinted polymer layer on the carbon dot-modified silica surface | [49] |
| DOX | 0.1–150 µM | 75.2 nM | polyethyleneimine-functionalized carbon dots (PEI-CDs) | [50] |
| DOX | 1–30 µM | 0.12 µM | Plum-based CDs | [51] |
| DOX | 86.2-17242 nM | 29 | Bell pepper-based CDs and Si@CdTe QDs for ratiometric detection | Present study |
| DAN | 1.773–113.477 µM | 177 nM | gold nanoparticles-multiwalled nanotubes-modified glassy carbon electrode (Au-MCNTs/GCE) | [52] |
| DAN | 200–5000 nM | 100 nM | 3D gold brush nanoelectrode ensembles (BNEEs) consisted of gold nanowires | [53] |
| DAN | 0.1 µM to 70 µM | 60 nM | an 808 nm-excited upconversion fuorescent sensor (CA-coated NaYF4:Yb/Er/Nd@NaYF4:Nd) | [54] |
| DAN | 0.26–16 µM | 70 nM | CdTe/CdS QDs | [25] |
| DAN | 33–88 nM | 19 nM | MUC1 aptamer-near infrared (NIR) $CuInS_2$ QDs | [55] |
| DAN | 54.37-8156.6 nM | 18.53 nM | Bell pepper-based CDs and Si@CdTe QDs for ratiometric detection | Present study |

# 3.6 Mechanism of fluorescent sensing

After incubation of drugs with CDs and Si@CdTe QDs system, the fluorescence intesity at 450 nm was quenched, while the intesity at 550 nm was constant. In this study for preventing the effect of drugs on the Si@CdTe QDs intesity and performance of ratiometric method, MSA-CdTe QDs were covered by silica layer. This event prevents direct interaction of anthraquinone drugs with MSA-CdTe QDs due to repulse of positive-charged amine groups of silica shell and positive-charged anthraquinone drugs leading to prevention of electron transfer from QDs to quinones and providing trustworthy reference signal for perfomance of ratiometric method [25, 56]. On the other side, the anthraquinone drugs of DOX and DAN can be considrably adsorbed on the negatively-charged CDs through electrostatic interaction followed by quenching of fluorescence intensity. As presented in Fig. 3**(H**) UV–vis absorbance spectra of DOX and DAN are located at 490 nm which mainly overlaped with fluorescence spectrum of CDs at 450 nm. Inner filter effect (IFE) is related to an event that the emission/excitation light of a fluorophore can be absorbed by an absorber due to a spectral overlaping between them [50]. So, the most possible mechanism for quenching of CDs fluorescence intensity by DOX and DAN is IFE phenomena.

# 3.7 Real sample

In order to evaluate the feasibility of the application of the introduced ratiometric method for DAN and DOX in serum matrix, different concentrations of drugs were incubated with CDs and Si@CdTeQDs in diluted serum for 40 minutes. The result of the investigation **(**Table 2) showed the applicability of the introduced RF sensor for the detection of DOX and DAN with a recovery of 86.32%-97.53% and 86.14%-99.62%, respectively. Moreover RSD (n = 3) for detection of DAN and DOX were 3.38%-1.48% and 3%-1.47%, respectively.

Table 2
The result of DOX and DAN measurement in the serum matrix.

| Drug | Added (nM) | Found (nM) | Recovery % | RSD % |
|---|---|---|---|---|
| DAN | 947.83 | 816.46 | 86.14 | 2.36 |
| | 3791.32 | 3362.14 | 88.68 | 3.02 |
| | 7582.65 | 6592.35 | 86.94 | 3.38 |
| | 9478.31 | 8874.54 | 93.63 | 1.69 |
| | 13269.6 | 13219.2 | 99.62 | 1.48 |
| DOX | 862.1 | 744.24 | 86.32 | 2.93 |
| | 3448.39 | 3002.33 | 87.06 | 2.42 |
| | 6896.79 | 6094.86 | 88.37 | 1.69 |
| | 8620.98 | 7812.03 | 90.61 | 3.03 |
| | 12069.38 | 11771.88 | 97.53 | 1.47 |

# 3.8 Intereference study

To identify the effect of the different interferes, which may present in the biological sample, on detection of 0.3 mg/L of drugs (0.286 mg/L DAN 543.77 nM and DOX 551.95 nM), the tolerance level of 5±% was considered as the limited range for changing the intensity of sensor signals [57]. As presented in Fig. 4 (**A and B**), the difference matrices containing $K_2CO_3$ (250 mg/L for DAN and 400 mg/L for DOX), Glutamine 250 mg/L, $KNO_3$ 500 mg/L, $Al_2(SO_4)_3$ $18H_2O$ 500 mg/L, Fructose 500 mg/L, Glucose 500 mg/L, $MgCl_2.6H_2O$ 500 mg/L, $CaCl_2$ 500 mg/L, NaCl (500 mg/L for DAN and 250 mg/L for DOX), $CuSO_4$ 500 mg/L and $Na_2HPO_4$ (500 mg/L DAN and 250 mg/L DOX) did not cause significant changes ( < ± 5%) in signal intensity. The maximum error percentage for detection of DAN and DOX was in the presence of 500 mg/L $CuSO_4$ (4.85%) and 400 mg/L $K_2CO_3$ (4.95%), respectively. These results demonstrated the high efficiency of RF sensor for detection of DAN and DOX.

# 3.9 Cell viability

The MTT assay as a colorimetric method was used to assess nanoparticles' cell metabolic activity and cytotoxicity [58]. The base of this test is the conversion of yellow tetrazolium dye MTT (3-(4, 5-dimethylthiazolyl-2)-2,5-diphenyltetrazolium bromide) to insoluble formazan ((E,Z)-5-(4,5-dimethylthiazol-2-yl)-1,3-diphenylformazan) by NAD(P)H-dependent cellular oxidoreductase enzyme [59]. The concentrations of 5-1500 mg/L CDs were incubated 24 hours with MCF-7 and PC3 cell lines, and according to results (Fig. 4C), minimum toxicity was observed on cell lines. Also, some *in-vivo* and *in-vitro* studies indicated that CDs have not negative effect on the biological parameters at reasonable concentration and can be considered as a safe and harmless alternative for biological uses in the future [60, 61]. So, according to the results (Fig. 4C**)** 600 mg/L was selected for imaging analysis.

# 3.10 Imaging analysis

Up to now living cells have been detected by fluorescent dyes and imaging techniques, while many of these dyes are toxic and cause cell death, or their fluorescence is weak and should be used in high concentrations [62]. So, the development of easy to synthesis and low toxicity agents is highly important for imaging. Because of their small size and unique property, CDs can quickly enter the cells and remained in them [63]. For this purpose CDs (600 ppm) with high safety were used as a fluorescent probe for cell imaging. As shown in Fig. 4 **(D and E)** CDs were observed in the cell membrane and cytoplasmic region without any damage to the cell nucleus [64], and the cells were easily imaged.

# 4. Conclusion

In this study, bell pepper-synthesized CDs and Si@CdTe QDs were successfully used for designing dual emission RF and detection of DAN and DOX in human samples. In presence of anthraquinone drugs, the intensity of CDs was quenched, while the intesity of Si@CdTe QDs was constant. So, a sensetive RF method was conducted to concidrablely detect DAN and DOX in serum sample whithot any significant interferences. The notable benefits such as eco-friendly, fast response time, high selectivity and sesitivity,

good precision and wide-ranging response, condidate preposed RF sesnor as a poetent technique for detection of anthraquinone drugs in biological samples. Furthermore greem-synthesized CDs successfully utilized for imaging of two important cell lines of PC3 and MCF-7. So, green and economical CDs can be a powerful altenative for commercial fluorescent dyes. Therefore, we can certainly claim that the green synthesized CDs has the best utilization outlook in the biological imaging and detection.

# Declarations


### Acknowledgement

The authors gratefully acknowledge the Vice Chancellor of Research of Mashhad University of Medical Sciences, Mashhad, Iran.


### Authers' contribution

The authors were involved in this project as follows:

Arash Mohammadnejad: methodology, formal analysis, writing, review, and manuscript editing. Sara Hamrah and Fereshteh Sanobari: methodology and investigation. Khalil Abnous and Morteza Alinejad Nameghi: conceptualization, supervision. Roghayeh Yahyazadeh: manuscript writing, formal analysis, software, and data curation. Seyed Ahmad Mohajery: conceptualization, supervision, data curation, funding acquisition, methodology, project administration, resources, validation, writing, review, and editing.


### Funding

This study supported by Vice Chancellor of Research of Mashhad University of Medical Sciences, Mashhad, Iran, through the grant numbers 971785 and 971760.


### Availability of data and materials

All data generated and analyzed during this research and included in this published article.

### Declaration of competing interest

The authors declare that they have no competing interests and agree for publication.

# References


1. Liu H, Ye T, Mao C: **Fluorescent carbon nanoparticles derived from candle soot.** *Angewandte Chemie International Edition* 2007, **46:**6473-6475.
2. Baker SN, Baker GA: **Luminescent carbon nanodots: emergent nanolights.** *Angewandte Chemie International Edition* 2010, **49:**6726-6744.

3. Wang J, Wang CF, Chen S: **Amphiphilic egg-derived carbon dots: Rapid plasma fabrication, pyrolysis process, and multicolor printing patterns.** *Angewandte Chemie International Edition* 2012, **51:**9297-9301.
4. Sun Y-P, Zhou B, Lin Y, Wang W, Fernando KS, Pathak P, Meziani MJ, Harruff BA, Wang X, Wang H: **Quantum-sized carbon dots for bright and colorful photoluminescence.** *Journal of the American Chemical Society* 2006, **128:**7756-7757.
5. Xu X, Ray R, Gu Y, Ploehn HJ, Gearheart L, Raker K, Scrivens WA: **Electrophoretic analysis and purification of fluorescent single-walled carbon nanotube fragments.** *Journal of the American Chemical Society* 2004, **126:**12736-12737.
6. Zhou J, Booker C, Li R, Zhou X, Sham T-K, Sun X, Ding Z: **An electrochemical avenue to blue luminescent nanocrystals from multiwalled carbon nanotubes (MWCNTs).** *Journal of the American Chemical Society* 2007, **129:**744-745.
7. Zhao XJ, Zhang WL, Zhou ZQ: **Sodium hydroxide-mediated hydrogel of citrus pectin for preparation of fluorescent carbon dots for bioimaging.** *Colloids and Surfaces B: Biointerfaces* 2014, **123:**493-497.
8. Ray S, Saha A, Jana NR, Sarkar R: **Fluorescent carbon nanoparticles: synthesis, characterization, and bioimaging application.** *The Journal of Physical Chemistry C* 2009, **113:**18546-18551.
9. Li H, He X, Liu Y, Huang H, Lian S, Lee S-T, Kang Z: **One-step ultrasonic synthesis of water-soluble carbon nanoparticles with excellent photoluminescent properties.** *Carbon* 2011, **49:**605-609.
10. Zhu H, Wang X, Li Y, Wang Z, Yang F, Yang X: **Microwave synthesis of fluorescent carbon nanoparticles with electrochemiluminescence properties.** *Chemical Communications* 2009**:**5118-5120.
11. Sahu S, Behera B, Maiti TK, Mohapatra S: **Simple one-step synthesis of highly luminescent carbon dots from orange juice: application as excellent bio-imaging agents.** *Chemical Communications* 2012, **48:**8835-8837.
12. Mehta VN, Jha S, Singhal RK, Kailasa SK: **Preparation of multicolor emitting carbon dots for HeLa cell imaging.** *New Journal of Chemistry* 2014, **38:**6152-6160.
13. Liu S-S, Wang C-F, Li C-X, Wang J, Mao L-H, Chen S: **Hair-derived carbon dots toward versatile multidimensional fluorescent materials.** *Journal of Materials Chemistry C* 2014, **2:**6477-6483.
14. Zhou J, Sheng Z, Han H, Zou M, Li C: **Facile synthesis of fluorescent carbon dots using watermelon peel as a carbon source.** *Materials Letters* 2012, **66:**222-224.
15. De B, Karak N: **A green and facile approach for the synthesis of water soluble fluorescent carbon dots from banana juice.** *Rsc Advances* 2013, **3:**8286-8290.
16. Wang L, Zhou HS: **Green synthesis of luminescent nitrogen-doped carbon dots from milk and its imaging application.** *Analytical chemistry* 2014, **86:**8902-8905.
17. Hsu P-C, Shih Z-Y, Lee C-H, Chang H-T: **Synthesis and analytical applications of photoluminescent carbon nanodots.** *Green Chemistry* 2012, **14:**917-920.

18. Wu L, Cai X, Nelson K, Xing W, Xia J, Zhang R, Stacy AJ, Luderer M, Lanza GM, Wang LV: **A green synthesis of carbon nanoparticles from honey and their use in real-time photoacoustic imaging.** *Nano research* 2013, **6:**312-325.
19. Li C-L, Ou C-M, Huang C-C, Wu W-C, Chen Y-P, Lin T-E, Ho L-C, Wang C-W, Shih C-C, Zhou H-C: **Carbon dots prepared from ginger exhibiting efficient inhibition of human hepatocellular carcinoma cells.** *Journal of Materials Chemistry B* 2014, **2:**4564-4571.
20. Prasannan A, Imae T: **One-pot synthesis of fluorescent carbon dots from orange waste peels.** *Industrial & Engineering Chemistry Research* 2013, **52:**15673-15678.
21. Kasibabu BSB, D'souza SL, Jha S, Singhal RK, Basu H, Kailasa SK: **One-step synthesis of fluorescent carbon dots for imaging bacterial and fungal cells.** *Analytical Methods* 2015, **7:**2373-2378.
22. Maniez-Devos DM, Baurain R, Lesne M, Trouet A: **Degradation of doxorubicin and daunorubicin in human and rabbit biological fluids.** *Journal of pharmaceutical and biomedical analysis* 1986, **4:**353-365.
23. Yang X, Gao H, Qian F, Zhao C, Liao X: **Internal standard method for the measurement of doxorubicin and daunorubicin by capillary electrophoresis with in-column double optical-fiber LED-induced fluorescence detection.** *Journal of pharmaceutical and biomedical analysis* 2016, **117:**118-124.
24. Jiang X, Feng D-Q, Liu G, Fan D, Wang W: **A fluorescent switch sensor for detection of anticancer drug and ctDNA based on the glutathione stabilized gold nanoclusters.** *Sensors and Actuators B: Chemical* 2016, **232:**276-282.
25. Li P, Liu S, Yan S, Fan X, He Y: **A sensitive sensor for anthraquinone anticancer drugs and hsDNA based on CdTe/CdS quantum dots fluorescence reversible control.** *Colloids and Surfaces A: Physicochemical and Engineering Aspects* 2011, **392:**7-15.
26. Kaushik D, Bansal G: **Characterization of degradation products of idarubicin through LC-UV, MSn and LC–MS-TOF studies.** *Journal of pharmaceutical and biomedical analysis* 2013, **85:**123-131.
27. Vajdle O, Zbiljić J, Tasić B, Jović D, Guzsvány V, Djordjevic A: **Voltammetric behavior of doxorubicin at a renewable silver-amalgam film electrode and its determination in human urine.** *Electrochimica Acta* 2014, **132:**49-57.
28. Liao LB, Zhou HY, Xiao XM: **Spectroscopic and viscosity study of doxorubicin interaction with DNA.** *Journal of molecular structure* 2005, **749:**108-113.
29. Breuzard G, Angiboust J-F, Jeannesson P, Manfait M, Millot J-M: **Surface-enhanced Raman scattering reveals adsorption of mitoxantrone on plasma membrane of living cells.** *Biochemical and biophysical research communications* 2004, **320:**615-621.
30. Liu S, Wang F, Liu Z, Hu X, Yi A, Duan H: **Resonance Rayleigh scattering spectra for studying the interaction of anthracycline antineoplastic antibiotics with some anionic surfactants and their analytical applications.** *Analytica chimica acta* 2007, **601:**101-107.
31. Yang X, Lin J, Liao X, Zong Y, Gao H: **Interactions between N-acetyl-L-cysteine protected CdTe quantum dots and doxorubicin through spectroscopic method.** *Materials Research Bulletin* 2015, **66:**169-175.

32. Dai C, Yang C-X, Yan X-P: **Ratiometric fluorescent detection of phosphate in aqueous solution based on near infrared fluorescent silver nanoclusters/metal–organic shell composite.** *Analytical chemistry* 2015, **87:**11455-11459.
33. Zhuang M, Ding C, Zhu A, Tian Y: **Ratiometric fluorescence probe for monitoring hydroxyl radical in live cells based on gold nanoclusters.** *Analytical chemistry* 2014, **86:**1829-1836.
34. Wang K, Qian J, Jiang D, Yang Z, Du X, Wang K: **Onsite naked eye determination of cysteine and homocysteine using quencher displacement-induced fluorescence recovery of the dual-emission hybrid probes with desired intensity ratio.** *Biosensors and Bioelectronics* 2015, **65:**83-90.
35. Singh NK, Chakma B, Jain P, Goswami P: **Protein-Induced Fluorescence Enhancement Based Detection of Plasmodium falciparum Glutamate Dehydrogenase Using Carbon Dot Coupled Specific Aptamer.** 2018, **20:**350-357.
36. Zhang Q, Liang J, Zhao L, Wang Y, Zheng Y, Wu Y, Jiang L: **Synthesis of Novel Fluorescent Carbon Quantum Dots From Rosa roxburghii for Rapid and Highly Selective Detection of o-nitrophenol and Cellular Imaging.** *Front Chem* 2020, **8:**665.
37. Mohammadinejad A, Es' haghi Z, Abnous K, Mohajeri SA: **Tandem determination of mitoxantrone and ribonucleic acid using mercaptosuccinic acid-capped CdTe quantum dots.** *Journal of Luminescence* 2017, **190:**254-260.
38. Mohammadinejad A, Taghdisi SM, Es' haghi Z, Abnous K, Mohajeri SA: **Targeted imaging of breast cancer cells using two different kinds of aptamers-functionalized nanoparticles.** *European Journal of Pharmaceutical Sciences* 2019, **134:**60-68.
39. Shi F, Liu S, Su X: **Dopamine functionalized-CdTe quantum dots as fluorescence probes for l-histidine detection in biological fluids.** *Talanta* 2014, **125:**221-226.
40. Gong Y, Fan Z: **Melamine-modulated mercaptopropionic acid-capped manganese doped zinc sulfide quantum dots as a room-temperature phosphorescence sensor for detecting clenbuterol in biological fluids.** *Sensors and Actuators B: Chemical* 2014, **202:**638-644.
41. Vibin M, Vinayakan R, John A, Raji V, Rejiya CS, Vinesh NS, Abraham A: **Cytotoxicity and fluorescence studies of silica-coated CdSe quantum dots for bioimaging applications.** *Journal of Nanoparticle Research* 2011, **13:**2587-2596.
42. Lu W, Xiaoyun Q, Liu S, Chang G, Zhang Y, Luo Y, Asiri AM, Al-youbi A, Sun X: **Economical, Green Synthesis of Fluorescent Carbon Nanoparticles and Their Use as Probes for Sensitive and Selective Detection of Mercury(II) Ions.** *Analytical chemistry* 2012, **84:**5351-5357.
43. Yin B, Deng J, Peng X, Long Q, Zhao J, Lu Q, Chen Q, Li H, Tang H, Zhang Y: **Green synthesis of carbon dots with down-and up-conversion fluorescent properties for sensitive detection of hypochlorite with a dual-readout assay.** *Analyst* 2013, **138:**6551-6557.
44. Lu W, Qin X, Liu S, Chang G, Zhang Y, Luo Y, Asiri AM, Al-Youbi AO, Sun XJAc: **Economical, green synthesis of fluorescent carbon nanoparticles and their use as probes for sensitive and selective detection of mercury (II) ions.** 2012, **84:**5351-5357.

45. Wolcott A, Gerion D, Visconte M, Sun J, Schwartzberg A, Chen S, Zhang JZ: **Silica-coated CdTe quantum dots functionalized with thiols for bioconjugation to IgG proteins.** *The Journal of Physical Chemistry B* 2006, **110:**5779-5789.
46. Hajian R, Tayebi Z, Shams N: **Fabrication of an electrochemical sensor for determination of doxorubicin in human plasma and its interaction with DNA.** *Journal of Pharmaceutical Analysis* 2017, **7:**27-33.
47. Alavi-Tabari SAR, Khalilzadeh MA, Karimi-Maleh H: **Simultaneous determination of doxorubicin and dasatinib as two breast anticancer drugs uses an amplified sensor with ionic liquid and ZnO nanoparticle.** *Journal of Electroanalytical Chemistry* 2018, **811:**84-88.
48. Chekin F, Myshin V, Ye R, Melinte S, Singh SK, Kurungot S, Boukherroub R, Szunerits S: **Graphene-modified electrodes for sensing doxorubicin hydrochloride in human plasma.** *Analytical and bioanalytical chemistry* 2019, **411:**1509-1516.
49. Xu Z, Deng P, Li J, Xu L, Tang S: **Molecularly imprinted fluorescent probe based on FRET for selective and sensitive detection of doxorubicin.** *Materials Science and Engineering: B* 2017, **218:**31-39.
50. Yang M, Yan Y, Liu E, Hu X, Hao H, Fan J: **Polyethyleneimine-functionalized carbon dots as a fluorescent probe for doxorubicin hydrochloride by an inner filter effect.** *Optical Materials* 2021, **112:**110743.
51. Zhu J, Chu H, Shen J, Wang C, Wei Y: **Green preparation of carbon dots from plum as a ratiometric fluorescent probe for detection of doxorubicin.** *Optical Materials* 2021, **114:**110941.
52. Li Q, Wu X, Zhao J, Wu C, Wang X: **Real-time detection of the interaction between anticancer drug daunorubicin and cancer cells by Au-MCNT nanocomposites modified electrodes.** *Science China Chemistry* 2011, **54:**812-815.
53. Cao L, Yan P, Sun K, Kirk DW: **Gold 3D brush nanoelectrode ensembles with enlarged active area for the direct voltammetry of daunorubicin.** *Electroanalysis: An International Journal Devoted to Fundamental and Practical Aspects of Electroanalysis* 2009, **21:**1183-1188.
54. Zeng J, Wang X, Jia Y, Mo J, Sun R, Wu T, Xu Q, Jin H: **A Fluorescent Sensor for Daunorubicin Determination Using 808 nm-excited Upconversion Nanoparticles.** *Journal of Inorganic and Organometallic Polymers and Materials* 2021.
55. Lin Z, Ma Q, Fei X, Zhang H, Su X: **A novel aptamer functionalized CuInS2 quantum dots probe for daunorubicin sensing and near infrared imaging of prostate cancer cells.** *Analytica chimica acta* 2014, **818:**54-60.
56. Wei J-R, Chen H-Y, Zhang W, Pan J-X, Dang F-Q, Zhang Z-Q, Zhang J: **Ratiometric fluorescence for sensitive and selective detection of mitoxantrone using a MIP@ rQDs@ SiO2 fluorescence probe.** *Sensors and Actuators B: Chemical* 2017, **244:**31-37.
57. Hashemzadeh N, Hasanzadeh M, Shadjou N, Eivazi-Ziaei J, Khoubnasabjafari M, Jouyban A: **Graphene quantum dot modified glassy carbon electrode for the determination of doxorubicin hydrochloride in human plasma.** *Journal of Pharmaceutical Analysis* 2016, **6:**235-241.

58. Almutary A, Sanderson BJ: **The MTT and Crystal Violet Assays: Potential Confounders in Nanoparticle Toxicity Testing.** *Int J Toxicol* 2016, **35:**454-462.
59. Bahuguna A, Khan I, Bajpai VK, Kang SCJBJoP: **MTT assay to evaluate the cytotoxic potential of a drug.** 2017, **12:**Online: Apr 8-2017.
60. Zhang S, Pei X, Xue Y, Xiong J, Wang J: **Bio-safety assessment of carbon quantum dots, N-doped and folic acid modified carbon quantum dots: A systemic comparison.** *Chinese Chemical Letters* 2020, **31:**1654-1659.
61. Zhao DL, Chung T-S: **Applications of carbon quantum dots (CQDs) in membrane technologies: A review.** *Water Research* 2018, **147:**43-49.
62. Zhu H, Fan J, Du J, Peng XJAoCR: **Fluorescent probes for sensing and imaging within specific cellular organelles.** 2016, **49:**2115-2126.
63. Kasibabu BSB, D'souza SL, Jha S, Singhal RK, Basu H, Kailasa SKJAM: **One-step synthesis of fluorescent carbon dots for imaging bacterial and fungal cells.** 2015, **7:**2373-2378.
64. Jung YK, Shin E, Kim B-S: **Cell nucleus-targeting zwitterionic carbon dots.** *Scientific reports* 2015, **5:**1-9.

# Scheme

Scheme 1 is available in the Supplementary Files section

# Figures

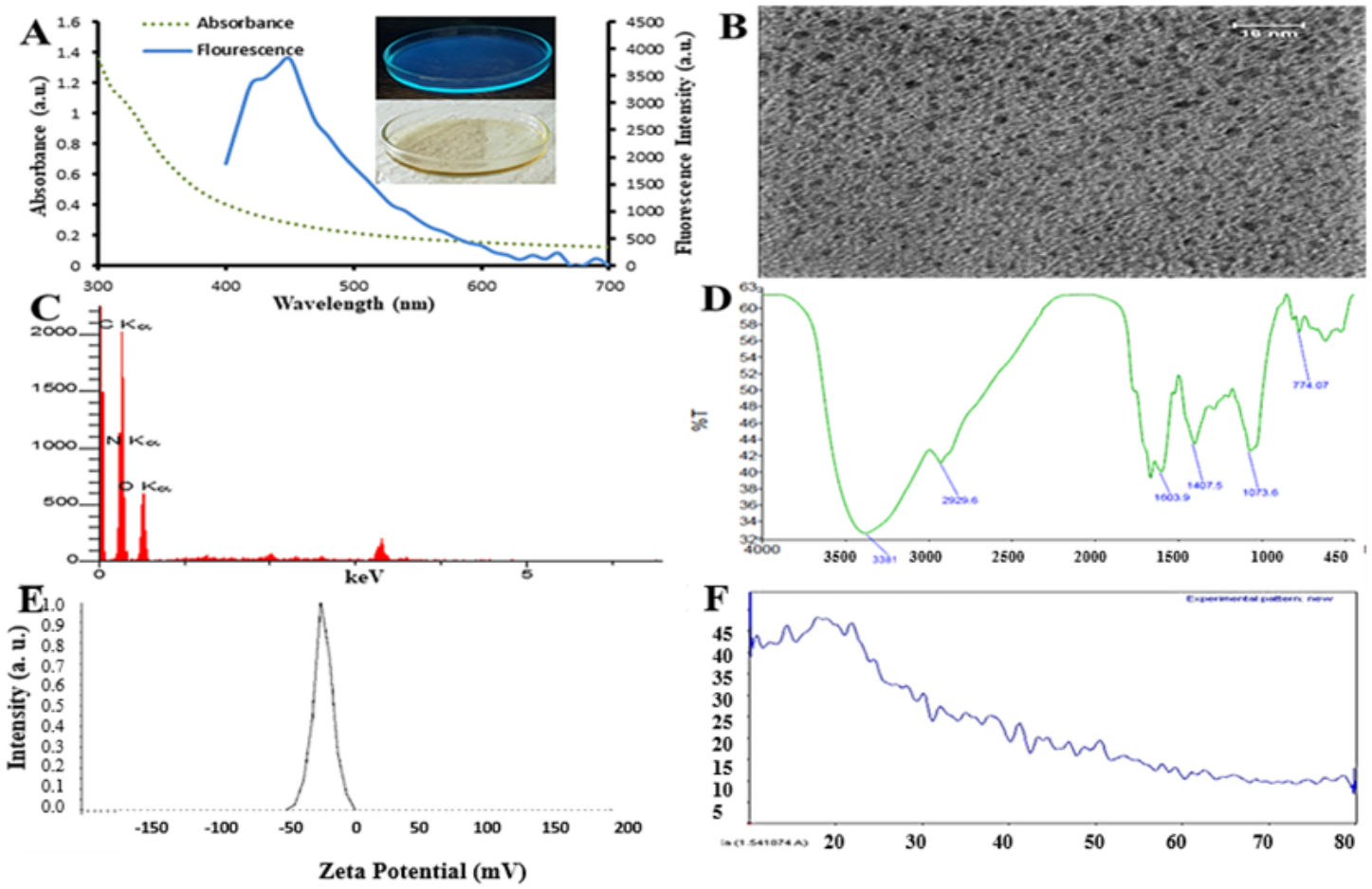


## Figure 1

Characterization of CDs by **(A)** UV-vis and fluorescence spectroscopy. Inset: CDs solution under UV (up) and room (down) light.; **(B)** TEM; **(C)** EDX; **(D)** FTIR; **(E)** DLS; **(F)** XRD.

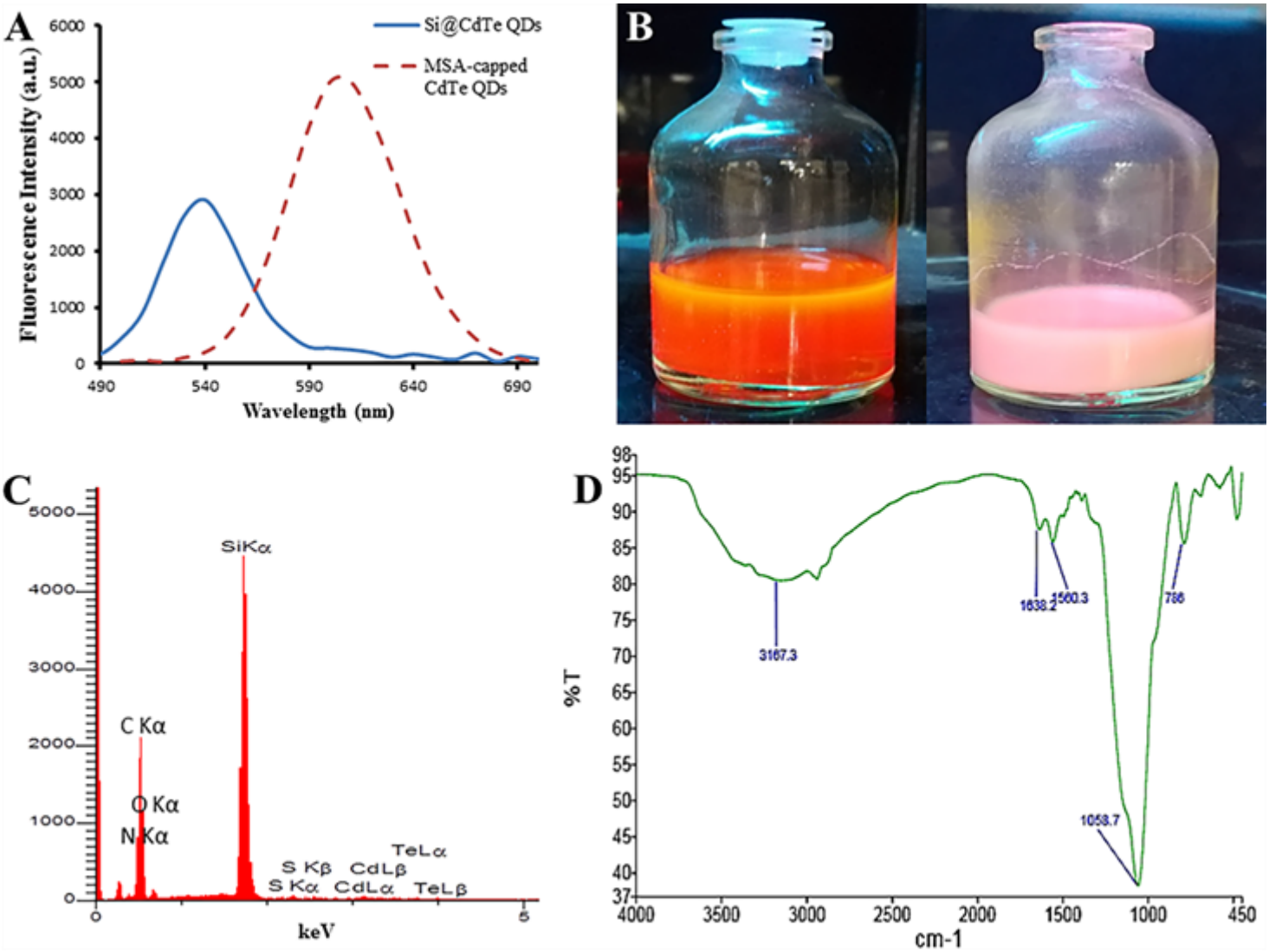


## Figure 2

Charactrization of Si@CdTe QDs by: **(A)** Fluorescence spectra ($\lambda_{exc=}$ 365 nm); **(B)** UV light radiation: left: MSA-capped CdTe QDs, Right: Si@CdTe QDs; **(C)** EDX; **(D)** FT-IR

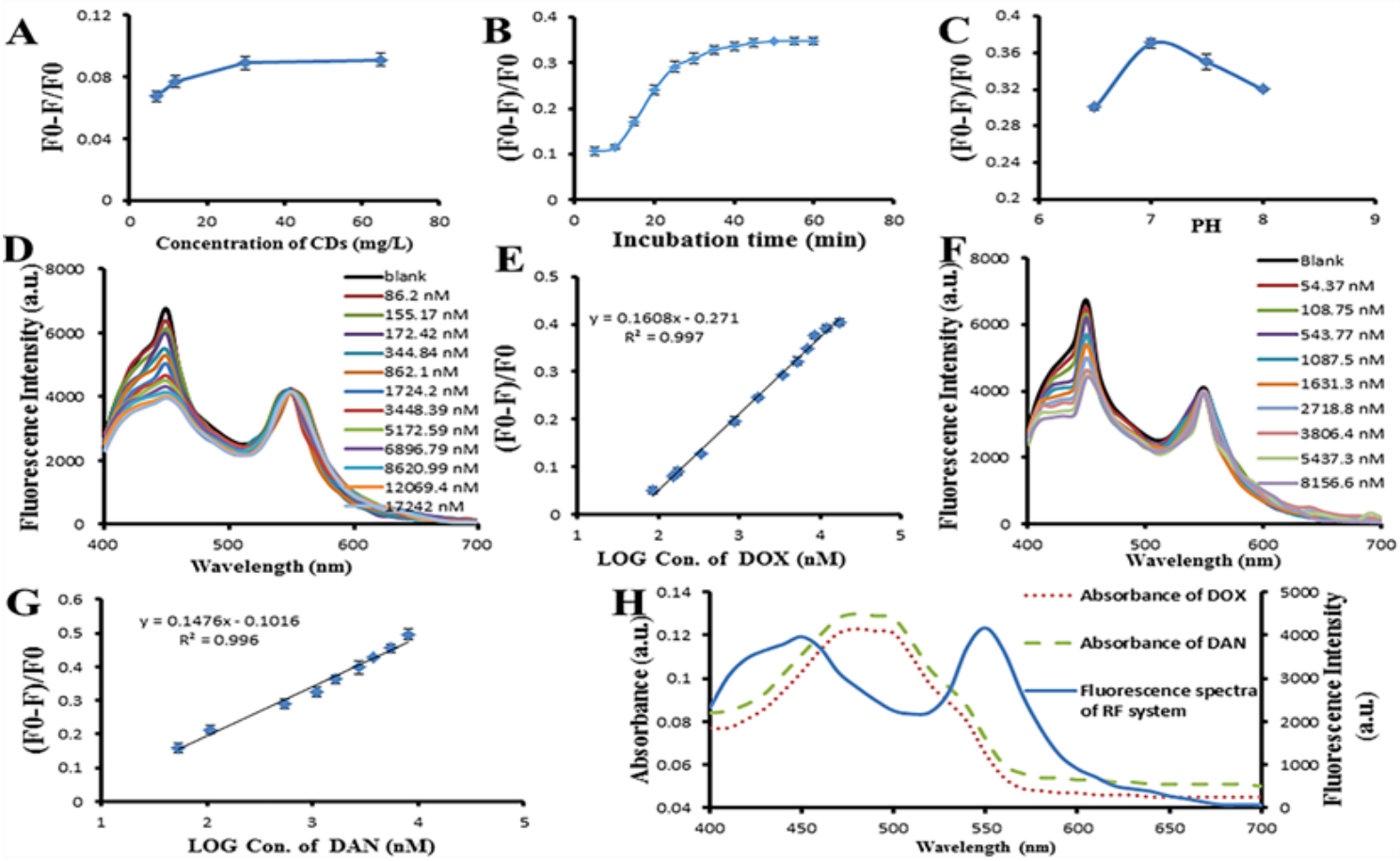


## Figure 3

**(A-C)** Optimization of conditions: **(A)** Concentration of CDs, **(B)** Incubation time, and **(C)** PH; **(D)** Fluorescence spectra of RF system in presence of different concentrations of DOX in range of 86.2-17242 nM; **(E)** Calibration curve of DOX detection; **(F)** Fluorescence spectra of RF system in presence of different concentrations of DAN in range of 54.37-8156.6 nM; **(G)** Calibration curve of DAN detection. Each point represents as mean±SD (n=3) **(H)** Overlaping of absorbance spectra of DOX and DAN with fluorescence spectra of RF system ($\lambda_{exc=}$ 365 nm).

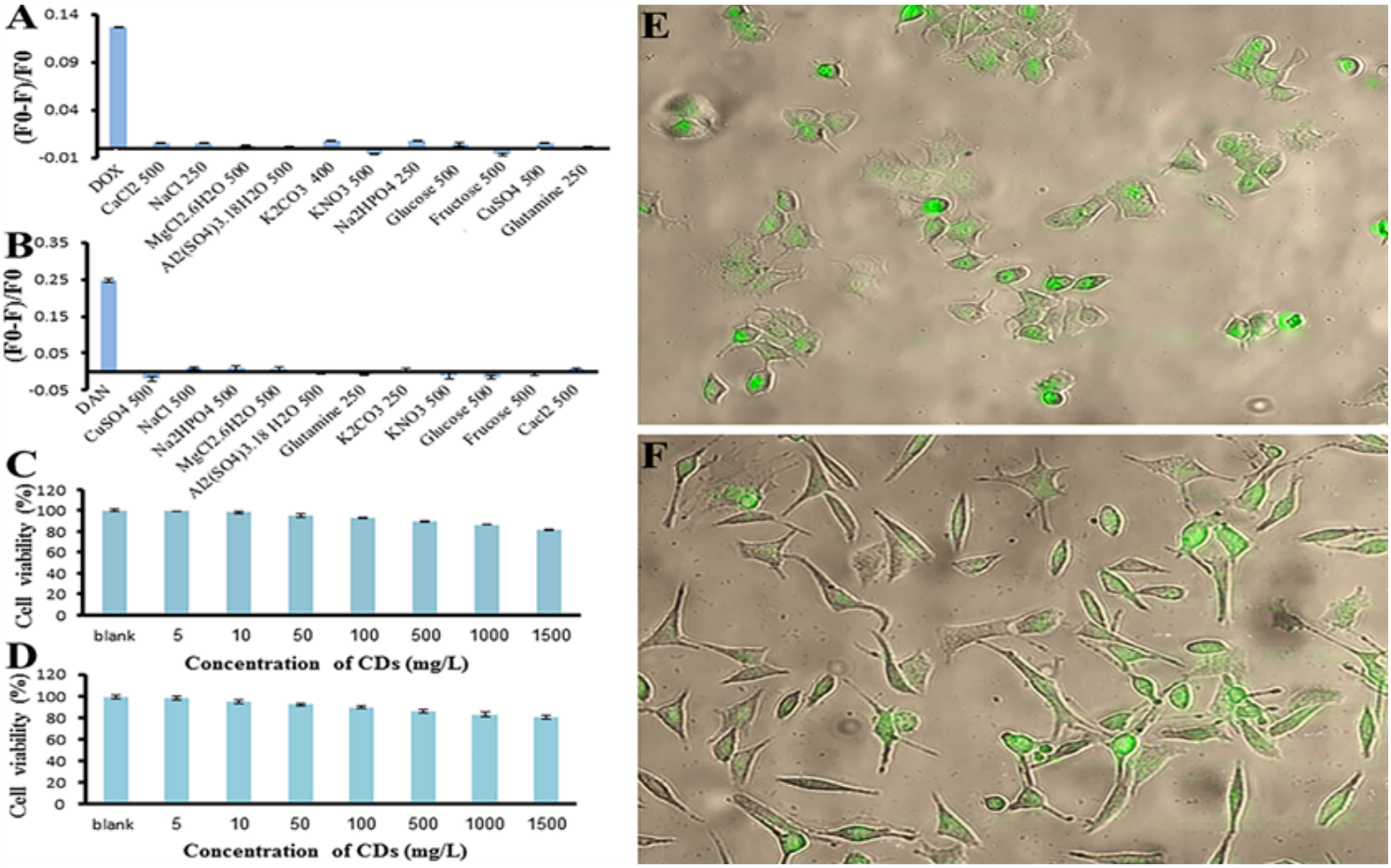


**Figure 4**

(**A, B**) Interference study for detection of: (**A**) DOX, and (**B**) DAN. Responses for interferers are presented as: Signal response in presence of interfere- Signal response in absence of interfere. ; (**C, D**) Results of MTT assay for evaluation of toxicity of CDs on: (**C**) MCF-7 and (**D**) PC3 cell lines. Each point represents as Means±SD (n=4) (**E, F**) Fluorescence imaging of: (**E**) MCF-7, (**F**) PC3 cell lines.

# Supplementary Files

This is a list of supplementary files associated with this preprint. Click to download.

- Scheme1.png
- GraphicalAbstarct.png